

1 Unpredictability of the fitness effects of antimicrobial resistance mutations across  
2 environments in *Escherichia coli*

3  
4 Aaron Hinz<sup>1,2,3\*</sup>, André Amado<sup>4,5,6</sup>, Rees Kassen<sup>2,3</sup>, Claudia Bank<sup>4,5,6</sup>, Alex Wong<sup>1</sup>

5  
6  
7 <sup>1</sup> Department of Biology, Carleton University, Ottawa, ON K1S 5B6, Canada

8 <sup>2</sup> Department of Biology, University of Ottawa, Ottawa, ON K1N 6N5, Canada

9 <sup>3</sup> Department of Biology, McGill University, Montreal, QC H3A 1B1, Canada

10 <sup>4</sup> Institute of Ecology and Evolution, University of Bern, Switzerland

11 <sup>5</sup> Swiss Institute of Bioinformatics, Lausanne, Switzerland

12 <sup>6</sup> Gulbenkian Science Institute, Oeiras, Portugal

13  
14 \* Corresponding author

15 Email: [aaron.hinz@mcgill.ca](mailto:aaron.hinz@mcgill.ca) (AH)

16  
17 Keywords: Antimicrobial Resistance, Costs of Resistance, Genotype-by-Environment

18 Interactions, Epistasis, Fitness Landscapes, Rough Mount Fuji Model

19





1 Andersson 2017). Second, some AMR mutations may incur little or no cost to the microbe,  
2 allowing resistance to be maintained in antibiotic-free environments (Melnyk et al. 2017). Third,  
3 costs might be heterogeneous across different environments, allowing for resistance to be  
4 maintained in cost-free environmental refuges (Leale and Kassen 2018). Finally, second-site  
5 compensatory mutations, either segregating in the population or arising after resistance  
6 evolution, can reduce fitness costs without loss of resistance (Durão et al. 2018).

7 Knowledge of the range of fitness effects caused by AMR mutations is crucial to guide  
8 decision-making but comprehensive data are lacking. Standard practice is to obtain experimental  
9 measures of the fitness effects of AMR mutations from well-characterized laboratory strains  
10 grown in standard growth media (Melnyk et al. 2015; Vogwill and MacLean 2015); however, it  
11 has become increasingly evident that these fitness effects can be modulated by both genetic and  
12 environmental variation (Hall 2013; Vogwill et al. 2016; Wong 2017; Clarke et al. 2020). For  
13 example, the magnitude or the direction (costly vs. beneficial) of a mutation's fitness effect may  
14 change depending on the genetic background in which the mutation evolved, a form of genotype  
15 by genotype (G x G) interaction known as epistasis (Trindade et al. 2009; Vogwill et al. 2016;  
16 Wong 2017). The growth environment can also impact fitness effects in ways that are hard to  
17 anticipate, a form of genotype by environment (G x E) interaction (Hall 2013; Maharjan and  
18 Ferenci 2017). Furthermore, higher-order interactions between the nature of the AMR mutation  
19 itself (modification of a target site versus deregulation of an efflux pump, for example), the  
20 genetic background on which the mutation occurs, and the growth environment (G x G x E  
21 interactions) can further complicate matters, potentially undermining predictions based on data  
22 from single genotypes and environments (Flynn et al. 2013; Hall 2013; Ghenu et al. 2023).  
23 Currently we know very little about the extent to which the fitness effects of AMR mutations are

1 consistent or variable across genotypes and environments. Obtaining such data is an important  
2 step towards predicting the success of antibiotic restriction strategies.

3       Ultimately, it will never be possible to empirically measure fitness for every mutation-  
4 genotype combination in all environments a microbial strain could encounter. Theoretical  
5 modeling could offer a complementary approach to predict the fitness of microorganisms across  
6 the various environments they populate. Two different types of models provide a rough  
7 prediction of antibiotic resistance fitness landscapes. Hill curve models predict fitness across  
8 antibiotic gradients but disregard other sources of environmental variation (Das et al. 2020).  
9 Alternatively, approaches based on Fisher's Geometric Model tend to have more general  
10 applicability, but have many parameters, require extensive datasets, and are in practice  
11 cumbersome to fit (Blanquart et al. 2014; Blanquart and Bataillon 2016; Harmand et al. 2017).  
12 Probabilistic fitness landscape models, such as the Rough Mount Fuji (RMF) model (Aita et al.  
13 2000), are a third type of model that capture the relationship between genotype and fitness.  
14 These models are appealing because they feature tunable epistasis and are determined by few  
15 parameters (Bank 2022). In addition, they reasonably approximate some experimental fitness  
16 landscapes (e.g., Bank et al. 2016).

17       In this study, we present an empirical analysis of genetic and environmental factors that  
18 contribute to the variation in fitness effects among resistance mutations in *Escherichia coli* and  
19 evaluate the performance of an RMF-based genotype-fitness model to reproduce the empirical  
20 results. We introduced 7 resistance mutations individually into each of 12, primarily clinical,  
21 strains and quantified each resistance mutation's fitness effect in four distinct growth  
22 environments. Overall, we show that fitness effects are extensively modulated by all three  
23 sources of variation: the type of AMR mutation, the genetic background, and the growth

1 environment. The RMF model reproduced single-environment empirical results well but was  
2 unable to recover their full complexity when all environments were considered together. Our  
3 study highlights the challenges of predicting fitness effects from empirical data obtained from  
4 limited genetic backgrounds and environments while at the same time calling for improved  
5 fitness landscape models that account for these important sources of variation.

## 7 **Results**

### 9 **Library of *E. coli* clinical isolates with introduced resistance** 10 **mutations**

12 We constructed a factorial mutant library by introducing each of 7 antimicrobial  
13 resistance mutations into 12 *E. coli* isolates using oligonucleotide-mediated mutagenesis (Lennen  
14 et al. 2016). The total number of mutant constructs was 67, after accounting for failed  
15 constructions and isolates that were resistant to the respective antibiotic or already harbored the  
16 mutation (fig. 1). The genetic backgrounds sampled were the laboratory strain MG1655 and 11  
17 clinical isolates, including enterohemorrhagic (EHEC) and extraintestinal pathogenic (ExPEC)  
18 *E. coli*, that vary in serotype, antibiotic resistance profile, and plasmid presence (Basra et al.  
19 2018; McCarthy 2020). For generalizability, we selected mutations that confer resistance to  
20 multiple antibiotic classes (fluoroquinolone, rifampicin, aminoglycoside) by modifying drug  
21 binding sites or by upregulating antibiotic efflux (Aleksun and Levy 1999; Nakamura et al.  
22 1989; Vila et al. 1994; Morgan-Linnell et al. 2009). Fitness effects of mutations in *gyrA*, *rpoB*,

1 and *rpsL* have been extensively characterized in *E. coli* reference strains (Trindade et al. 2009;  
2 Trindade et al. 2012; Durão et al. 2015), but not in clinical isolates. Mutations in the selected  
3 genes contribute to clinical resistance in *E. coli* (*gyrA*, *marR*) and other pathogens such as  
4 *Pseudomonas aeruginosa* and *Mycobacterium tuberculosis* (*gyrA*, *gyrB*, *rpoB*, *rpsL*) (Sreevatsan  
5 et al. 1996; Hopkins et al. 2005; Lee et al. 2005; Goldstein 2014; Melnyk et al. 2015; Huseby et  
6 al. 2017; Bhatnagar and Wong 2019). Overall, the mutant library includes a range of AMR  
7 mutations causing resistance to multiple antibiotic types introduced in genetic backgrounds that  
8 sample the genomic diversity of pathogenic *E. coli* populations found in nature.

## 9

### 10 **Mutations cause similar increases in antibiotic resistance across *E.*** 11 ***coli* genetic backgrounds**

12

13 We expected the mutants to exhibit increased resistance to antibiotics whose inhibitory  
14 action or efflux was directly impacted by the introduced mutation. However, indirect effects of  
15 the mutations against non-target antibiotics (i.e., cross-resistance or collateral sensitivity), and  
16 the extent to which antibiotic susceptibilities depended on the genetic background were  
17 unknown. We therefore performed minimum inhibitory concentration (MIC) assays to quantify  
18 fold-changes in susceptibility to both target and non-target antibiotics (fig. 2). We found that the  
19 introduced mutations significantly increased resistance to target antibiotics across the genetic  
20 backgrounds. Thus, fluoroquinolone resistance mutations (in *gyrA*, *gyrB*, and *marR*) increased  
21 ciprofloxacin resistance, *rpoB* mutations increased rifampicin resistance, and *rpsL* mutations  
22 increased streptomycin resistance. Although several instances of collateral sensitivity were  
23 observed, none were significant when considering all genetic backgrounds.





1 2001; Polzin et al. 2013). The growth yields of the environments varied, with an over 10-fold  
2 change in carrying capacity between the highest yield (LB) and lowest yield (synthetic urine)  
3 media (supplementary fig. S2). Fitness effects were estimated by calculating the fitness of each  
4 mutant relative to its unmutated ancestor, thus allowing for comparisons between mutants  
5 generated from different genetic backgrounds.

6 The fitness effects of the studied AMR mutations are summarized in fig. 3, where  
7 individual points in each boxplot represent different genetic backgrounds sharing the same  
8 mutation. The mutations were generally costly (with relative fitness  $< 1$ ); however, there was  
9 wide variation in the fitness effects across genetic backgrounds including neutral and,  
10 surprisingly, even beneficial effects. This variation contrasts with the antibiotic susceptibility  
11 phenotypes, which varied little across genetic backgrounds (fig. 2). The dependence of the  
12 fitness effects on the genetic background is evidence of epistasis between AMR mutations and  
13 genetic backgrounds, a type of G X G interaction.

14 We summarized the fitness effects for all combinations of the focal mutations and genetic  
15 backgrounds in each environment with three statistics: (1) the mean fitness effects across  
16 mutations and genetic backgrounds; (2) the overall variance in fitness effects; and (3) the amount  
17 of epistasis between mutations and genetic backgrounds (fig. 4). Epistasis was estimated using  
18 the summary statistic gamma ( $\gamma$ ), defined as the correlation of fitness effects of the set of AMR  
19 mutations across multiple genetic backgrounds (Ferretti et al. 2016). We found that despite  
20 similar mean fitness effects (between -0.06 and -0.092), the variance of the fitness effects and  
21 amount of epistasis varied considerably depending on the growth environment. Fitness effect  
22 variance was much larger in the media mimicking the infection environments (synthetic urine  
23 and synthetic colon media), whereas epistasis was stronger (i.e., there was a lower correlation of

1 fitness effects across genetic backgrounds) for synthetic urine and M9-Glucose media, compared  
2 to synthetic colon and LB media. Despite differences in the total strength of epistasis, the four  
3 environments exhibited roughly similar proportions of epistasis types (supplementary fig. S4),  
4 with ~60-70% classified as magnitude epistasis, in which the genetic background affects fitness  
5 non-additively in the same direction, and ~30-40% as sign epistasis, in which the genetic  
6 background affects the direction of the fitness effect (e.g., deleterious to beneficial or vice versa).  
7 Taken together, our results demonstrate the important role of epistasis in determining fitness  
8 effects of AMR mutations and, furthermore, the influence of the growth environment on both the  
9 overall variation in fitness effects and strength of epistasis between mutations and genetic  
10 backgrounds.

## 11

### 12 **Variation in fitness effects is governed by irreducible G x E**

### 13 **interactions**

## 14

15 The experimental fitness data highlight the dramatic influence of the growth environment  
16 on the fitness effects of AMR mutations. Changing the growth environment can lead to  
17 differences in fitness that depend on both the identity of the mutation and the genetic background  
18 (fig. 3). For example, the *gyrB* mutation was highly costly in synthetic colon medium but less  
19 costly (and sometimes beneficial) in synthetic urine medium. The *gyrA* and *marR* mutations, on  
20 the other hand, exhibited the opposite response in these two environments. These results  
21 demonstrate that the impact of growth environments on fitness can vary from mutation to  
22 mutation (i.e., mutation by environment interaction).



## 1 **The complex G x G x E interactions in the experimental data are not** 2 **captured by a probabilistic fitness landscape model**

3  
4 Our dataset provides a powerful test case for investigating the predictability of mutational  
5 fitness effects. For example, given data from one environment, can we predict the fitness effects  
6 of AMR mutations in a second environment? In the previous section we showed that the data  
7 exhibit strong variation in fitness effects and epistasis within and between environments,  
8 indicating ubiquitous G x G and G x E interactions (figs. 4 and 5). Would such variation be  
9 expected under a simple fitness landscape model, and would the data be consistent with the same  
10 fitness landscape being sampled independently for each of the environments? If yes, this  
11 indicates that at least statistical properties of the data (such as the variance in fitness effects and  
12 epistasis) are predictable, even in the absence of detailed mechanistic knowledge of the cellular  
13 and physiological effects. We chose the Rough-Mount-Fuji (RMF) model (Aita et al. 2000) to  
14 address this question due to its success in describing single environment fitness landscapes and  
15 its reliance on few parameters (Szendro et al. 2013; Bank et al. 2016). The model considers a  
16 genotype as a set of alleles at diallelic loci, which each contribute additively to fitness, plus a  
17 random epistatic component, specific to each genotype, which also contributes to fitness. The  
18 model can be tuned from completely additive to completely epistatic by adjusting the  
19 distributions from which the additive and epistatic components of fitness are drawn.

20 To test whether the experimental data were consistent with an underlying RMF fitness  
21 landscape, we simulated a total of 100,000 fitness landscapes with 7 diallelic loci on 12 different  
22 genetic backgrounds (i.e., 84 genotypes) for 10,000 sets of model parameters ( $\sigma_a$  and  $\sigma_b$ ),





1 correlation observed between synthetic urine and synthetic colon media fitness effects was  
2 driven by a combination of positive and negative mutation-specific correlations, suggesting that  
3 genetic backgrounds associated with higher costs in synthetic urine medium were associated with  
4 reduced costs in synthetic colon medium and vice versa.

5 Variation in the strength of correlation between environments is indicative of mutation by  
6 genetic background by environment (G x G x E) interactions. Mutations with high correlations in  
7 fitness effects can be considered to have low levels of genetic background by environment (G x  
8 E) interaction, i.e., different genetic backgrounds respond similarly to both environments. On the  
9 other hand, a low correlation indicates high levels of G x E interaction, i.e., environmental  
10 effects on fitness depend on the genetic background. By this logic, the differences in correlations  
11 that we observe between mutations are indicators of G x G x E interactions, since the level of G  
12 x E interaction changes depending on the mutation. Although our sampling of genetic  
13 backgrounds is too sparse to make strong claims about mutation-level correlations, the variation  
14 in correlation coefficients that we observe in fig. 7B further supports that G x G x E interactions  
15 underlie the AMR mutation fitness effects.

## 17 **Genetic background fitness and phylogenetic relatedness are poor** 18 **predictors of fitness effects**

19  
20 Although the experimental data show that genetic background is a significant source of  
21 variation on AMR fitness effects, further information about the isolates might help untangle the  
22 genetic background effects. We investigated whether two properties of the genetic backgrounds

1 might explain the variation in fitness effects: their comparative relative fitness in each  
2 environment, and their phylogenetic relatedness. Beneficial mutations are expected to have  
3 smaller effect sizes for starting genotypes closer to a fitness peak (i.e., well-adapted to the  
4 growth medium) than genotypes further from the peak (Wang et al. 2016) . However, less is  
5 known about the expected magnitude of fitness effects for deleterious mutations at different  
6 distances from the peak (Diaz-Colunga et al. 2023). Therefore, we investigated whether any  
7 correlation existed between the starting fitness of the genetic backgrounds and the fitness effects  
8 of the introduced AMR mutations. We estimated genetic background fitness in each of the four  
9 growth environments by competing each of the 12 unmutated isolates against a common  
10 competitor (supplementary fig. S8A). We observed some variation in the background fitness of  
11 the isolates, suggesting that some genotypes were better adapted to each growth environment  
12 than others. However, apart from a weak positive correlation in the M9-Glucose environment  
13 (fig. 8A; supplementary fig. S9), we found no evidence that background fitness could predict the  
14 fitness effects of AMR mutations.

15 We also tested whether phylogenetic relatedness could predict differences in fitness  
16 effects observed between genetic backgrounds. We reasoned that closely related genetic  
17 backgrounds would be more likely to share mutations that interact with the introduced AMR  
18 mutations, and would hence exhibit more similar fitness effects. We constructed a whole-genome  
19 maximum-likelihood phylogeny of our genetic backgrounds, from which we calculated genetic  
20 distances between all pairs of strains. We found weak positive correlations between differences  
21 in fitness effects and genetic distance for the M9-Glucose and synthetic urine media (fig. 8B),  
22 but no correlation for the LB and synthetic colon media. Interestingly, a subset of mutations was  
23 responsible for the positive correlations observed for the M9-Glucose and synthetic urine media



1 (supplementary fig. S10). Nevertheless, despite these exceptions, our analysis suggests that  
2 genetic background fitness and phylogenetic relatedness were poor overall predictors of AMR  
3 mutation fitness effect variation.  
4

## 5 **Discussion**

6  
7 The predictability of evolutionary processes depends crucially on the impact of  
8 environmental and genetic variation on the fitness effects of mutations. Given the threat of  
9 antimicrobial resistance (AMR) to human health, knowledge of the factors determining the  
10 fitness effects of AMR mutations has important implications for antimicrobial stewardship. To  
11 the extent that resistance mutations are generally costly, antibiotic restriction is expected to  
12 reduce the prevalence of resistance. However, if costs of resistance are highly variable because  
13 they depend on environment and/or genetic background, then resistance might persist in  
14 favorable environmental or genetic refuges. Thus, we sought to measure, and ultimately predict,  
15 the effects of genetic background and environment on the fitness of AMR mutants.

16 We systematically measured the fitness effects of 7 resistance mutations across a range of  
17 *E. coli* genetic backgrounds and environments. The 12 genetic backgrounds included a standard  
18 laboratory strain and 11 clinical isolates, and the four growth environments included standard  
19 laboratory media, as well as media designed to mimic important sites of infection for *E. coli*.  
20 AMR mutations caused fairly uniform increases in resistance itself (fig. 2) and were on average  
21 costly in the absence of antibiotics (fig. 3). However, the magnitudes of their impacts on fitness  
22 were highly variable (fig. 3). Importantly, these fitness effects could not be predicted simply by  
23 knowing the identity of the resistance mutation, but instead depended to varying degrees on the

1 assay environment, the genetic background of the host strain, and interactions between individual  
2 terms. These complex interactions rendered the fitness effects of resistance mutations highly  
3 unpredictable.

4 Genotype-by-environment interactions are well documented in the quantitative and  
5 evolutionary genetics literature. Across a broad range of organisms, mutations may have  
6 drastically different effects in different environments (reviewed in Des Marais et al. 2013; Rauw  
7 and Gomez-Raya 2015). Likewise, there is growing evidence that AMR mutations, although  
8 typically deleterious, can have widely varying fitness effects depending on the environmental  
9 context (Trindade et al. 2012; Durão et al. 2015; Gifford et al. 2016; Clarke et al. 2020). We  
10 similarly find that the fitness effects of resistance mutations depend on the assay environment – a  
11 given mutation may be deleterious in some environments but neutral on average in others (fig. 3,  
12 GyrB (D426N)), or even beneficial in some environments but not others (e.g., the beneficial  
13 effect of MarR (R77H) in synthetic colon medium). Although not the focus of the study, several  
14 genotype-by-environment interactions we observed have biologically plausible mechanisms  
15 based on the presence of specific constituents or nutritional complexity of the media. For  
16 example, *marR* mutations, which cause elevated expression of the AcrAB-TolC multidrug efflux  
17 pump (Oethinger et al. 1998; Alekshun and Levy 1999; Barbosa and Levy 2000), could be  
18 beneficial in synthetic colon medium due to increased efflux of bile salts, a known substrate of  
19 the pump (Rosenberg et al. 2003). Similarly, differential fitness effects of RpoB (H526Y)  
20 mutations are thought to reflect alterations to global transcription that are beneficial specifically  
21 during growth in nutritionally poor media (Conrad et al. 2010).

22 In addition to widespread G x E, we found that the fitness effects of AMR mutations  
23 depend on genetic context. In contrast to the relatively uniform effects of the mutations on

1 resistance (fig. 2), the fitness effects in the absence of antibiotics could be deleterious, neutral, or  
2 beneficial depending on the genetic background. Our results reinforce the conclusions of  
3 empirical studies demonstrating the influence of genetic background on AMR fitness costs  
4 (Wong 2017). Trindade et al. (Trindade et al. 2009) observed widespread epistasis among AMR  
5 mutations in *E. coli*, with combinations of resistance mutations introduced in the same genetic  
6 background frequently exhibiting non-additive fitness effects. Similarly, but at a larger  
7 phylogenetic scale, Vogwill et al. (2016) identified large variation in the costs of rifampicin-  
8 resistance mutations across 8 different species within the genus *Pseudomonas*, with much of the  
9 variance attributed to the interaction between mutation and genetic background. Taken together,  
10 these experimental studies suggest that the costs of AMR are strongly influenced by epistatic  
11 interactions between AMR mutations and other loci over broad scales of relatedness, ranging  
12 from single nucleotide to strain and species level differences.

13 Our multi-factorial study design also allowed us to detect three-way interactions between  
14 mutation, background genotype, and environment (fig. 7). Here, different resistance mutations  
15 demonstrate contrasting G x E interactions. For example, fitness effects across genetic  
16 backgrounds are well correlated for MarR (R77H) between synthetic urine and M9-Glucose  
17 media (i.e., low G x E), but not for RpoB (H526Y) (i.e., high G x E). Relatedly, we also find that  
18 overall levels of epistasis between mutations and genetic backgrounds differ from one  
19 environment to another (fig. 4C). Crucially, G x G x E interactions make it difficult to predict  
20 costs of resistance between environments, implying that mutation-genotype combinations will  
21 respond idiosyncratically to a change in environment. Thus, estimates of fitness using standard  
22 lab strains or growth environments may be poor predictors of fitness in clinical settings, limiting  
23 our ability to predict which types of resistance will respond to antibiotic restriction, and how

1 quickly they will do so. Furthermore, although resistance (as measured by MIC) was similar  
2 across genotypes, resistance was only assessed in LB medium, and it is possible that growth in  
3 alternative growth environments could reveal G x E interactions undermining this predictability.

4 The complex gene by environment interactions underpinning the mutational fitness  
5 effects in our experimental dataset provided a test case for the ability of a fitness landscape  
6 model to statistically reproduce the observed patterns in the data. For this purpose, we chose one  
7 of the simplest probabilistic fitness landscape models, the Rough Mount Fuji (RMF) model,  
8 which features tunable epistasis with few parameters and thus lends itself as a base model to test  
9 hypotheses regarding the consequences of epistasis in evolution (Bank 2022). Although the RMF  
10 model does not incorporate any explicit expectations of how a fitness landscape may differ  
11 between environments, its probabilistic nature results in a large variation of fitness landscapes  
12 that can be produced under the same parameters. Therefore, we tested 1) how well the model  
13 could fit the data of each single environment, and 2) whether it could accommodate the data  
14 from all environments with the same set of parameters. We found that the RMF model was able  
15 to fit the statistics of individual environments well (fig. 6), considering the variation in fitness  
16 effects observed across genetic backgrounds. The model parameters suggest substantial epistasis  
17 for all environments, with the standard deviation of the epistatic contribution to the fitness  
18 effects typically larger than the standard deviation of the mean additive contribution. Although  
19 the RMF model could accommodate the fitness effect statistics for each environment separately,  
20 we found that no set of parameters could successfully explain the same statistics when all  
21 environments were considered together. In other words, the fitness landscapes in different  
22 environments could not be described as independent draws from a model with common  
23 parameters. We conclude that because even the most general features of the underlying fitness

1 landscape (i.e., the average additive and epistatic contributions to fitness) are irreconcilable  
2 between environments, successful prediction of fitness will require sophisticated models that  
3 incorporate additional, environment-specific factors.

4 The failure of our RMF-like model to predict fitness across environments raised the question  
5 of what additional information would be required. We investigated two possibilities here –  
6 phylogenetic relatedness, and relative fitness of the ancestral genotypes. Phylogenetic relatedness  
7 could in principle help to predict epistatic interactions, since closely related genotypes share  
8 more polymorphisms than distant relatives. The fitness effects of focal resistance mutations  
9 should be similar for close relatives to the extent that these effects are modulated by these shared  
10 polymorphisms. However, we found no correlation between relatedness and the fitness effects of  
11 resistance mutations (fig. 8B). One potential explanation for this lack of correlation is that  
12 different mutations which interact with our focal resistance mutations arise so frequently that  
13 they are not shared even between closely related genotypes. It is also possible that complex  
14 genetic interactions between mutations modulate fitness effects such that phylogenetic  
15 relatedness may not provide enough resolution to be predictive.

16 Alternatively, the fitness effects of a mutation may not be determined by specific interactions  
17 with other mutations in a given genetic background, but rather by global properties of a  
18 genotype. Fitness is a clear candidate for such a property – in the widely observed phenomenon  
19 of ‘diminishing returns’ epistasis, beneficial mutations confer a smaller gain for genotypes with  
20 higher starting fitness (Khan et al. 2011; Kryazhimskiy et al. 2014; Perfeito et al. 2014; Wang et  
21 al. 2016). Wang et al. (2016), for example, provided clear evidence that the fitness effects of  
22 several beneficial mutations were predicted well by the fitness of the ancestral genotype, but not  
23 by relatedness or by metabolic similarity. Likewise, there is some theoretical and empirical



1 fitness effects was driven more by differences in the magnitudes of the costs rather than changes  
2 in sign from costly to beneficial (supplementary fig. S4). Thus, to the extent that our findings  
3 translate to clinical settings, we would expect antibiotic restriction interventions to be successful  
4 on average in reducing the prevalence of resistance, but at an unpredictable pace. Furthermore,  
5 some mutations were more consistently costly across environments and genetic backgrounds  
6 (i.e., RpsL (K43R) and RpoB (S531L)), suggesting that knowledge of the mutation could  
7 provide some level of predictive value for antibiotic restriction outcomes. In addition, our study  
8 calls for the further development of fitness landscape models across environments and their  
9 evaluation in the light of data such as those presented in this study. Such models could help  
10 identify the variables that influence predictability and inform subsequent experimental study  
11 design.

12

## 13 **Materials and Methods**

14

### 15 **Bacterial strains, growth conditions, and antibiotics**

16

17 The *E. coli* isolates sampled for AMR mutagenesis include the K-12 reference strain  
18 (MG1655) (Blattner et al. 1997), six extra-intestinal isolates collected from patients during the  
19 2007-11 CANWARD survey of antibiotic-resistant pathogens in Canada (Zhanel et al. 2013;  
20 Basra et al. 2018), and three enterohemorrhagic strains from the Ottawa Laboratory Carling













1 blanks. The following antibiotics and two-fold concentration ranges were tested: ciprofloxacin  
2 (0.003125 to 204.8  $\mu\text{g/ml}$ ), rifampicin (3.125 to 3200  $\mu\text{g/ml}$ ), and streptomycin (3.125 to 3200  
3  $\mu\text{g/ml}$ ). MICs for each of the antibiotics were determined for all 67 AMR mutants and their 12  
4 ancestors in three replicate assays inoculated from the same overnight cultures. Two *rpoB*  
5 mutants [PB4 RpoB (H526Y) and PB15 RpoB (S531L)] and all except one *rpsL* mutant [PB13  
6 RpsL (K43R)] grew at the maximum tested concentrations (3200  $\mu\text{g/ml}$ ) of rifampicin and  
7 streptomycin, respectively. Their MICs (6400  $\mu\text{g/ml}$ ) should be considered lower-bound  
8 estimates, and therefore, variation in streptomycin resistance among *rpsL* mutants was not  
9 accurately determined. Plots show the median fold change in MIC due to mutation for the three  
10 replicate estimates (calculated by dividing the MIC of the mutant by the median MIC of the  
11 ancestor).

12 Differences in antibiotic susceptibility caused by the introduced mutations across  
13 different genetic backgrounds were determined by a multiple comparison t-test in R Version  
14 4.2.2 (R Core Team 2021) with the `compare_means` function in the `ggpubr` package. Median  
15 fold-changes in MIC ( $\log_2$ -transformed) were compared between mutants and ancestors (with  
16 antibiotic as a grouping variable) and significance was assessed using Bonferroni-adjusted p-  
17 values. The predictability of MIC fold increases was determined by fitting a mixed-effect linear  
18 model using the `lmer` function in the `lme4` package. The model predicts the fold-change in MIC  
19 ( $\log_2$ -transformed) for target antibiotics from the identity of the introduced mutation (fixed  
20 effect), with the genetic background and interaction between genetic background and mutation  
21 included as random effects. Correlations between MIC fold-increases and ancestral MIC were  
22 determined using `stat_cor` in the `ggpubr` package.

23

## 1 **Growth media and carrying capacity estimates**

2  
3 Competition experiments were performed in lysogeny broth (LB), M9-Glucose, synthetic  
4 urine medium, and synthetic colon medium. LB and M9-Glucose were prepared as described  
5 (Sambrook and Russell 2001). Synthetic urine medium is a defined medium containing 416 mM  
6 urea and 10 mM creatinine and was modified from published recipes (Laube et al. 2001; Clarke  
7 2018) by the addition of 0.001% Casamino acids to augment bacterial growth. Synthetic colon  
8 medium is a tryptone-based medium supplemented with 0.4% bile salts and was prepared as  
9 described (Polzin et al. 2013). The concentrations of each media component and details on  
10 preparation are found in supplementary tables S3, S4, S5, and S6.

11 The carrying capacity was assessed for each ancestral isolate following 20 h of growth in  
12 each competition growth medium. Isolates were inoculated in duplicate in LB broth and  
13 incubated 24 h at 37 °C with shaking. Cultures were diluted (1:100) into each of the competition  
14 growth media (LB, M9-Glucose, synthetic urine medium, and synthetic colon medium) and  
15 incubated 24 h for media acclimation. Acclimated cultures were diluted (1:100) into fresh  
16 competition growth media and incubated for 24 h. Growth yields were determined by plating  
17 serial dilutions of the cultures on LB agar, and calculating the number of colony forming units  
18 per ml.



1 Coulter) with a minimum of 20,000 counts per sample. Fluorescence was detected using the 488  
 2 nm excitation laser and 525/40 nm detection filter. Numbers of fluorescent and non-fluorescent  
 3 cells were estimated using Kaluza analysis software. Signal thresholds for distinguishing  
 4 fluorescent from non-fluorescent cells were established for each YFP-marked genotype by  
 5 analyzing pure cultures of marked and unmarked strains. To distinguish cells from non-specific  
 6 particles, gates were drawn in forward vs. side scatter plots that maximized the proportion of  
 7 YFP-positive counts in pure cultures. The number of unmarked cells in each sample were  
 8 estimated by subtracting the number of YFP-positive gated counts from the total number of gated  
 9 counts.

## 11 **Relative fitness calculations**

13 Relative fitness ( $\omega$ ) was calculated as previously described (Melnik et al. 2015) from the  
 14 initial ( $i$ ) and final ( $f$ ) counts of the unmarked focal ( $n1$ ) and marked competitor ( $n2$ ) strains and  
 15 the number of generations (estimated as 6.64 as described above):

$$17 \quad \omega = 1 + \frac{\ln\left(\frac{n1_f}{n1_i}\right) - \ln\left(\frac{n2_f}{n2_i}\right)}{\text{No. of generations}} \quad (\text{Eq. 1})$$

18 To account for fitness effects caused by the YFP marker or use of a non-isogenic competitor, the  
 19 relative fitness value for each AMR mutant was divided by the relative fitness of its wild-type  
 20 ancestor (competed against the same YFP-marked strain). These scaled fitness values, therefore,  
 21 indicate the effects of the introduced AMR mutations alone. The common competitor MG1655-  
 22 YFP was used for competitions involving genetic backgrounds OLC809, PB2, PB5, PB6, and



1 PB10. In control experiments, we determined that MG1655-YFP was a valid common  
 2 competitor since strong negative interactions were not observed between MG1655-YFP and the  
 3 5 ancestral strains (supplementary fig. S11). Furthermore, similar relative fitness trends were  
 4 observed in competitions regardless of whether an isogenic or common competitor was used  
 5 (supplementary fig. S12).

6 Variance component analysis of the relative fitness estimates was performed in R using  
 7 the lmer function in the lme4 package. For each mutation, a random effects model was fit that  
 8 included genetic background, environment, and their interaction as random factors contributing  
 9 to variance in relative fitness. The plots show the fitness effects variance explained by each  
 10 random effect, as well as the proportion of total variance explained.

## 12 **Epistasis analysis**

14 To quantify epistasis, we used the gamma statistic ( $\gamma$ ), introduced by (Ferretti et al. 2016).  
 15  $\gamma$  is defined as the average correlation of fitness effects across diverse genetic backgrounds in  
 16 which a mutation manifests. This can be mathematically expressed as

$$17 \gamma = \frac{\sum_g \sum_{g' \neq g} \sum_i s_i(g) \cdot s_i(g')}{(L - 1) \sum_g \sum_i s_i^2(g)}, \quad (\text{Eq. 2})$$

18 where  $g$  and  $g'$  index all possible genotypes,  $i$  all existing mutations, and  $s_i(g)$  represents the  
 19 effect of mutation  $i$  in the  $g$  background.

20 When the correlation is close to 1, the effect of the mutations is relatively consistent  
 21 across the genetic backgrounds they appear, implying minimal epistasis. As the value of  $\gamma$



1 where  $a_i \sim \mathcal{N}(\mu_a, \sigma_a)$  and  $b(g) \sim \mathcal{N}(0, \sigma_b)$ ; i.e., the additive contributions  $a_i$  of each locus  $i$   
 2 follow a normal distribution with mean  $\mu_a$  and standard deviation  $\sigma_a$  and the epistatic  
 3 components  $b(g)$  follow a normal distribution with zero mean and standard deviation  $\sigma_b$ . Each  
 4 allele  $g_i$  takes the values one or zero, indicating the state of locus  $i$  in genotype  $g$ , with a value  
 5 of one denoting a resistance mutation present in the genotype and the value of zero marking the  
 6 absence of a resistance mutation at that locus.

7 This model produces a fitness effect  $s_j(i)$  of a mutation  $i$  in a background  $j$  given by

$$8 \quad s_j(i) = f(g_{[i]}) - f(g) = a_i + b(g_{[i]}) - b(g) \quad (\text{Eq. 4})$$

9 where  $g$  is the genotype of the background  $j$  and  $g_{[i]}$  the genotype of the background with the  
 10 mutation in locus  $i$ .

11 To compare the model's predictions to the data, we constructed a fine grid of pairs of  $\sigma_a$   
 12 and  $\sigma_b$ , for  $\sigma_{a/b} \in [0, 0.24]$  with intervals of 0.002. We assumed the mean fitness effect in the  
 13 model, represented by the parameter  $\mu_a$ , to be equal to the mean of the experimentally measured  
 14 fitness effects. For each of these pairs, we generated  $10^6$  instances of the model and calculated  
 15 three summary statistics of the landscape: the mean of fitness effects, the variance of fitness  
 16 effects, and the gamma epistasis parameters. We used this generated data to obtain the  
 17 distribution of each summary statistic.

18 With these distributions, we estimated the likelihood of obtaining the data statistics given  
 19 the set of model parameters for each summary statistic. In the plots, the likelihood values are  
 20 represented relative to the maximum likelihood, so all log-likelihoods shown have a maximum of  
 21 0.



$$\begin{cases} \mu_a = \bar{\mu}, \\ \sigma_a = \sqrt{\sigma_s^2 - (1 - \bar{\gamma})(\bar{\mu}^2 + \sigma_s^2)}, \\ \sigma_b = \sqrt{(1 - \bar{\gamma})(\bar{\mu}^2 + \sigma_s^2)/2}, \end{cases} \quad (\text{Eq. 6})$$

2 which corresponds to an estimate of the best model parameters based only on the experimental  
 3 mean values of the statistics. These provide good estimates for the best parameters for the case of  
 4 single environment landscapes, but fail to describe multiple environment landscapes because the  
 5 distribution of the statistics is not well approximated by their mean value.

## 7 **Analysis of genetic relatedness**

8 A whole-genome phylogeny was generated using the REALPHY webserver (Bertels et al. 2014)  
 9 (<https://realphy.unibas.ch/realphy/>). FASTA formatted genome sequences were uploaded and  
 10 aligned to the reference K-12 (MG1655) sequence using Bowtie2 (Langmead and Salzberg  
 11 2012) with default parameters. A maximum likelihood tree was then inferred using PhyML  
 12 (Guindon et al. 2010), again with default parameters.

## 14 **Acknowledgements**

16 This study was funded by a JPI-AMR grant to AW, RK, and CB (Canadian Institutes of Health  
 17 Research grant no. 150766, FCT grant JPIAMR/0001/2016). AA was supported by ERC Starting  
 18 Grant 804569 (FIT2GO) to CB. CB acknowledges support by SNF project grant  
 19 315230\_204838/1 (MiCo4Sys).



- 1 Basra P, Alsaadi A, Bernal-Astrain G, O’Sullivan ML, Hazlett B, Clarke LM, Schoenrock A, Pitre S,  
2 Wong A. 2018. Fitness Tradeoffs of Antibiotic Resistance in Extraintestinal Pathogenic  
3 *Escherichia coli*. *Genome Biol Evol.* 10:667–679.
- 4 Bertels F, Silander OK, Pachkov M, Rainey PB, van Nimwegen E. 2014. Automated reconstruction of  
5 whole-genome phylogenies from short-sequence reads. *Mol Biol Evol.* 31:1077–1088.
- 6 Bhardwaj P, Hans A, Ruikar K, Guan Z, Palmer KL. 2017. Reduced Chlorhexidine and Daptomycin  
7 Susceptibility in Vancomycin-Resistant *Enterococcus faecium* after Serial Chlorhexidine  
8 Exposure. *Antimicrob Agents Chemother.* 62:e01235-17.
- 9 Bhatnagar K, Wong A. 2019. The mutational landscape of quinolone resistance in *Escherichia coli*. *PLOS*  
10 *One.* 14:e0224650.
- 11 Blanquart F, Achaz G, Bataillon T, Tenaillon O. 2014. Properties of selected mutations and genotypic  
12 landscapes under Fisher’s geometric model. *Evolution.* 68:3537–3554.
- 13 Blanquart F, Bataillon T. 2016. Epistasis and the Structure of Fitness Landscapes: Are Experimental  
14 Fitness Landscapes Compatible with Fisher’s Geometric Model? *Genetics.* 203:847–862.
- 15 Blattner FR, Plunkett G, Bloch CA, Perna NT, Burland V, Riley M, Collado-Vides J, Glasner JD, Rode  
16 CK, Mayhew GF, et al. 1997. The Complete Genome Sequence of *Escherichia coli* K-12.  
17 *Science.* 277:1453–1462.
- 18 Blomfield IC, Vaughn V, Rest RF, Eisenstein BI. 1991. Allelic exchange in *Escherichia coli* using the  
19 *Bacillus subtilis sacB* gene and a temperature-sensitive pSC101 replicon. *Mol Microbiol.* 5:1447–  
20 1457.





- 1 Des Marais DL, Hernandez KM, Juenger TE. 2013. Genotype-by-Environment Interaction and Plasticity:  
2 Exploring Genomic Responses of Plants to the Abiotic Environment. *Annu Rev Ecol Evol Syst.*  
3 44:5–29.
- 4 Diaz-Colunga J, Skwara A, Gowda K, Diaz-Uriarte R, Tikhonov M, Bajic D, Sanchez A. 2023. Global  
5 epistasis on fitness landscapes. *Philos Trans R Soc B.* 378:20220053.
- 6 Dierikx CM, Hengeveld PD, Veldman KT, de Haan A, van der Voorde S, Dop PY, Bosch T, van  
7 Duijkeren E. 2016. Ten years later: still a high prevalence of MRSA in slaughter pigs despite a  
8 significant reduction in antimicrobial usage in pigs the Netherlands. *J Antimicrob Chemother.*  
9 71:2414–2418.
- 10 Durão P, Balbontín R, Gordo I. 2018. Evolutionary Mechanisms Shaping the Maintenance of Antibiotic  
11 Resistance. *Trends Microbiol.* 26:677–691.
- 12 Durão P, Trindade S, Sousa A, Gordo I. 2015. Multiple Resistance at No Cost: Rifampicin and  
13 Streptomycin a Dangerous Liaison in the Spread of Antibiotic Resistance. *Mol Biol Evol.*  
14 32:2675–2680.
- 15 Ellis HM, Yu D, DiTizio T, Court DL. 2001. High efficiency mutagenesis, repair, and engineering of  
16 chromosomal DNA using single-stranded oligonucleotides. *Proc Natl Acad Sci U S A.* 98:6742–  
17 6746.
- 18 Enne VI. 2010. Reducing antimicrobial resistance in the community by restricting prescribing: can it be  
19 done? *J Antimicrob Chemother.* 65:179–182.
- 20 Enne VI, Livermore DM, Stephens P, Hall LM. 2001. Persistence of sulphonamide resistance in  
21 *Escherichia coli* in the UK despite national prescribing restriction. *Lancet.* 357:1325–1328.





- 1 Laube N, Mohr B, Hesse A. 2001. Laser-probe-based investigation of the evolution of particle size  
2 distributions of calcium oxalate particles formed in artificial urines. *J Cryst Growth*. 233:367–  
3 374.
- 4 Leale AM, Kassen R. 2018. The emergence, maintenance, and demise of diversity in a spatially variable  
5 antibiotic regime. *Evolution Letters*. 2:134–143.
- 6 Lebeuf-Taylor E, McCloskey N, Bailey SF, Hinz A, Kassen R. 2019. The distribution of fitness effects  
7 among synonymous mutations in a gene under directional selection. *eLife*. 8:e45952.
- 8 Lee JK, Lee YS, Park YK, Kim BS. 2005. Alterations in the GyrA and GyrB subunits of topoisomerase II  
9 and the ParC and ParE subunits of topoisomerase IV in ciprofloxacin-resistant clinical isolates of  
10 *Pseudomonas aeruginosa*. *Int J Antimicrob Agents*. 25:290–295.
- 11 Lennen RM, Nilsson Wallin AI, Pedersen M, Bonde M, Luo H, Herrgård MJ, Sommer MOA. 2016.  
12 Transient overexpression of DNA adenine methylase enables efficient and mobile genome  
13 engineering with reduced off-target effects. *Nucleic Acids Res*. 44:e36.
- 14 Maharjan R, Ferenci T. 2017. The fitness costs and benefits of antibiotic resistance in drug-free  
15 microenvironments encountered in the human body. *Environ Microbiol Rep*. 9:635–641.
- 16 McCarthy A. 2020. Identification of Hypermutator Enterohemorrhagic *Escherichia coli* (EHEC) Using a  
17 High Throughput Screening Method to Inform Food Safety Investigations. Available from:  
18 <https://repository.library.carleton.ca/concern/etds/qr46r1659>
- 19 Melnyk AH, McCloskey N, Hinz AJ, Dettman J, Kassen R. 2017. Evolution of Cost-Free Resistance  
20 under Fluctuating Drug Selection in *Pseudomonas aeruginosa*. *mSphere*. 2:e00158-17.
- 21 Melnyk AH, Wong A, Kassen R. 2015. The fitness costs of antibiotic resistance mutations. *Evol Appl*.  
22 8:273–283.

- 1 Morgan-Linnell SK, Becnel Boyd L, Steffen D, Zechiedrich L. 2009. Mechanisms accounting for  
2 fluoroquinolone resistance in *Escherichia coli* clinical isolates. *Antimicrob Agents Chemother.*  
3 53:235–241.
- 4 Nakamura S, Nakamura M, Kojima T, Yoshida H. 1989. *gyrA* and *gyrB* mutations in quinolone-resistant  
5 strains of *Escherichia coli*. *Antimicrob Agents Chemother.* 33:254–255.
- 6 Oethinger M, Podglajen I, Kern WV, Levy SB. 1998. Overexpression of the *marA* or *soxS* Regulatory  
7 Gene in Clinical Topoisomerase Mutants of *Escherichia coli*. *Antimicrob Agents Chemother.*  
8 42:2089–2094.
- 9 Perfeito L, Sousa A, Bataillon T, Gordo I. 2014. Rates of Fitness Decline and Rebound Suggest Pervasive  
10 Epistasis. *Evolution.* 68:150–162.
- 11 Pitiriga V, Vrioni G, Saroglou G, Tsakris A. 2017. The Impact of Antibiotic Stewardship Programs in  
12 Combating Quinolone Resistance: A Systematic Review and Recommendations for More  
13 Efficient Interventions. *Adv Ther.* 34:854–865.
- 14 Polzin S, Huber C, Eylert E, Elsenhans I, Eisenreich W, Schmidt H. 2013. Growth Media Simulating Ileal  
15 and Colonic Environments Affect the Intracellular Proteome and Carbon Fluxes of  
16 Enterohemorrhagic *Escherichia coli* O157:H7 Strain EDL933. *Appl Environ Microbiol.* 79:3703–  
17 3715.
- 18 R Core Team. 2021. R: A Language and Environment for Statistical Computing. Available from:  
19 <https://www.R-project.org/>
- 20 Rakowski SA, Filutowicz M. 2013. Plasmid R6K replication control. *Plasmid.* 69:231–242.
- 21 Rauw WM, Gomez-Raya L. 2015. Genotype by environment interaction and breeding for robustness in  
22 livestock. *Front Genet.* 6:310.





1 Zhanel GG, Adam HJ, Baxter MR, Fuller J, Nichol KA, Denisuik AJ, Lagacé-Wiens PRS, Walkty A,  
2 Karlowsky JA, Schweizer F, et al. 2013. Antimicrobial susceptibility of 22746 pathogens from  
3 Canadian hospitals: results of the CANWARD 2007-11 study. *J Antimicrob Chemother.* 68 Suppl  
4 1:i7-22.

5

## 6 **Figure Legends**

7

8 **Fig 1. Library of *E. coli* isolates with introduced AMR mutations.** The gene and specific  
9 amino acid change of the 7 introduced mutations are indicated. The mutations confer resistance  
10 to three antibiotic classes and alter the indicated cellular targets. The 12 *E. coli* genetic  
11 backgrounds include a common laboratory strain (MG1655) and 11 clinical isolates collected  
12 from patients in Canadian hospitals. 67 of the 84 potential mutation-by-genotype combinations  
13 were successfully constructed. 13 combinations were not attempted due to elevated resistance of  
14 the ancestor to the respective antibiotic (Resistant), and four combinations were unsuccessfully  
15 introduced (NA). PB10, PB13, and PB15 already harbored both S83L and D87N mutations in  
16 *gyrA*, likely contributing to elevated fluoroquinolone resistance. No other isolates carried known  
17 resistance mutations in the genes under investigation.

18

19 **Fig 2. Mutations introduced in different genetic backgrounds consistently increase**  
20 **resistance to target antibiotics.** Median fold-changes in antibiotic susceptibility [ $\log_2$  ( $MIC_{mutant}$   
21 /  $MIC_{ancestor}$ )] are plotted for mutants with introduced (A) fluoroquinolone, (B) rifampicin, and  
22 (C) aminoglycoside resistance mutations. MICs were determined for three antibiotics (one target  
23 and two non-target) in triplicate. Individual points within each category represent different



1 genetic backgrounds with the same introduced mutation. Each of the mutations significantly  
2 increased resistance to target antibiotics across genetic backgrounds (multiple comparison t-test  
3 with Bonferroni correction;  $p_{\text{adj}} < 0.05$ ) with no significant effects on susceptibility to off-target  
4 antibiotics. The collateral streptomycin sensitivity observed for the RpoB (H526Y) mutants was  
5 not significant when adjusting for multiple comparisons ( $p_{\text{adj}} = 0.54$ ).

6

7 **Fig 3. AMR mutations exhibit wide variation in fitness effects across genetic backgrounds.**

8 The fitness effects of AMR mutations were determined in four antibiotic-free environments: LB,  
9 M9-Glucose, synthetic urine medium, and synthetic colon medium. The data are grouped by  
10 mutation and environment, with individual points indicating fitness effects measured in different  
11 genetic backgrounds. The boxplots summarize the distributions of fitness effects (median, first  
12 and third quartiles, and nonoutlier minimum and maximum values). Additional fitness effect  
13 information including genetic background identities, relative fitness values, and significance  
14 levels is provided in supplementary fig. S3.

15

16 **Fig 4. Fitness effects variance and epistasis between AMR mutations and genetic**

17 **backgrounds differed between environments.** The overall mean (A) and variance (B) of  
18 fitness effects of all mutation-genetic background combinations (67 mutants) were determined in  
19 each growth environment. Global epistasis (C) was estimated as gamma epistasis. Analysis of  
20 the amount and proportion of epistasis types (i.e., magnitude vs. sign epistasis) underlying the  
21 epistasis measure are found in supplementary fig. S4.

22

1 **Fig 5. Genotype by environment interactions explain most of the variation in fitness effects**  
2 **for each AMR mutation.** The experimental fitness effects data for each mutation was fit to a  
3 random effects model to determine the amount (A) and proportion (B) of variance explained by  
4 Genotype (i.e., the genetic background), Environment, and the Genotype by Environment  
5 interaction. Reaction norm plots showing the responses of specific genotypes in each  
6 environment are found in supplementary fig. S5.

7  
8 **Fig 6. A Rough Mount Fuji genotype-fitness model only partially reproduces the**  
9 **experimental fitness effect statistics.** (A) Log-likelihood surfaces for the mean of fitness  
10 effects, the variance of fitness effects, and the gamma epistasis parameter of the experimental  
11 data under a RMF model. x-axis represents the variance of the additive component ( $\sigma_a$ ) and y-  
12 axis the variance of the epistatic contribution ( $\sigma_b$ ). Each row shows log-likelihood surfaces for  
13 single environments and the last row for the conjugation of the four environments. The red dot  
14 represents an analytical estimate of the best parameters based on the mean values of the  
15 experimental data statistics only. The mean of the additive fitness effects (model parameter  $\mu_a$ )  
16 was fixed to the experimentally measured mean. (B) The RMF model cannot simultaneously  
17 capture the distribution of the variance of fitness effects and the epistasis for the four  
18 environments. The figure shows the distribution of the mean of fitness effects, the variance of  
19 fitness effects, and the gamma parameter under a RMF model. The top row represents a RMF  
20 landscape with parameters optimized to describe the variance of fitness effects and the bottom  
21 row optimized to describe the gamma parameter. The vertical colored lines represent the  
22 experimental value for each environment, with the dashed lines delimiting one standard



**Resistance mutations**

<b>Ancestors</b>		Fluoroquinolone			Rifampicin		Aminoglycoside	
		DNA gyrase		Efflux pump	RNA polymerase		Ribosomal protein	
		GyrA (S83L, D87N)	GyrB (D426N)		RpoB (H526Y)	RpoB (S531L)	RpsL (K43T)	RpsL (K43R)
				MarR (R77H)				
Reference strain	MG1655							
Enterohemorrhagic strains	OLC682							
	OLC809							
	OLC969		NA				Resistant	Resistant
Urinary tract isolates	PB1					NA		
	PB2							
	PB4					NA		
	PB5							
	PB6		NA				Resistant	Resistant
	PB10	Resistant	Resistant	Resistant				
	PB13	Resistant	Resistant	Resistant				
Respiratory isolate	PB15	Resistant	Resistant	Resistant				

Figure 1  
110x76 mm (x DPI)

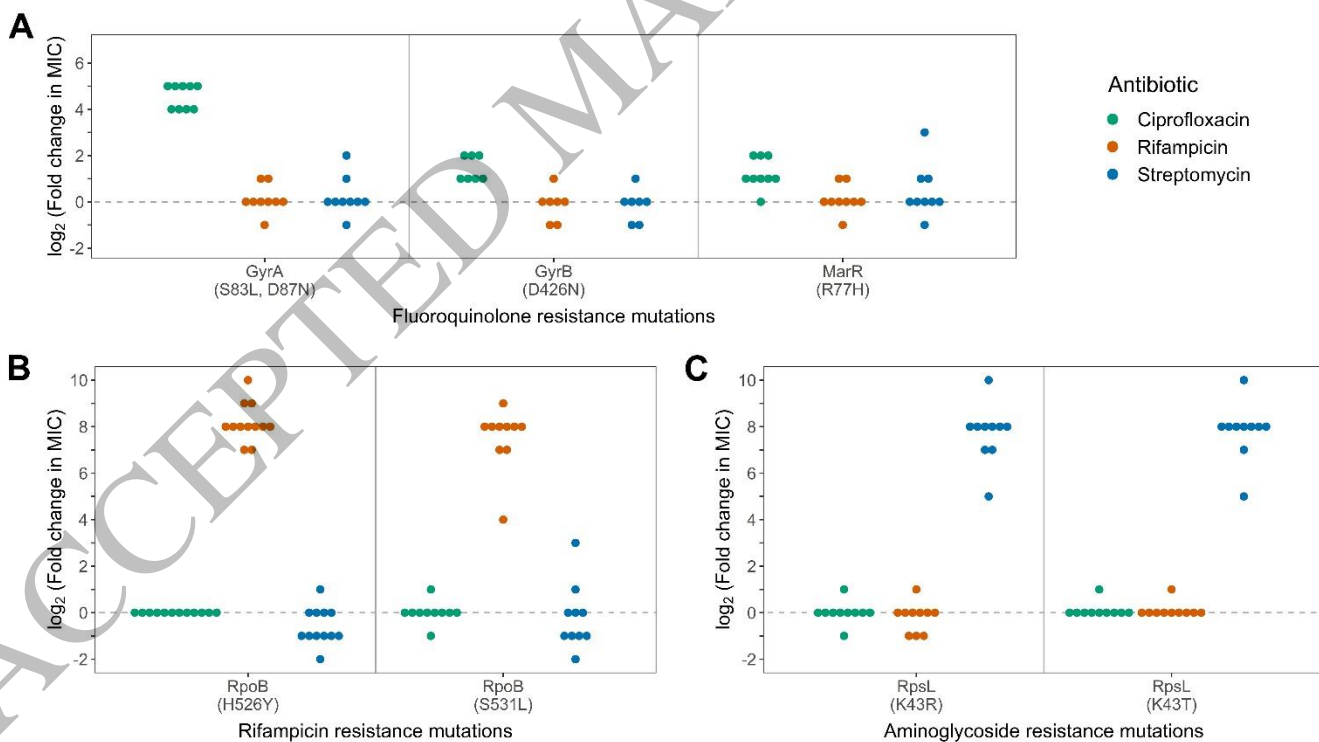


Figure 2  
182x104 mm (x DPI)

1  
2  
3  
4

5  
6  
7  
8

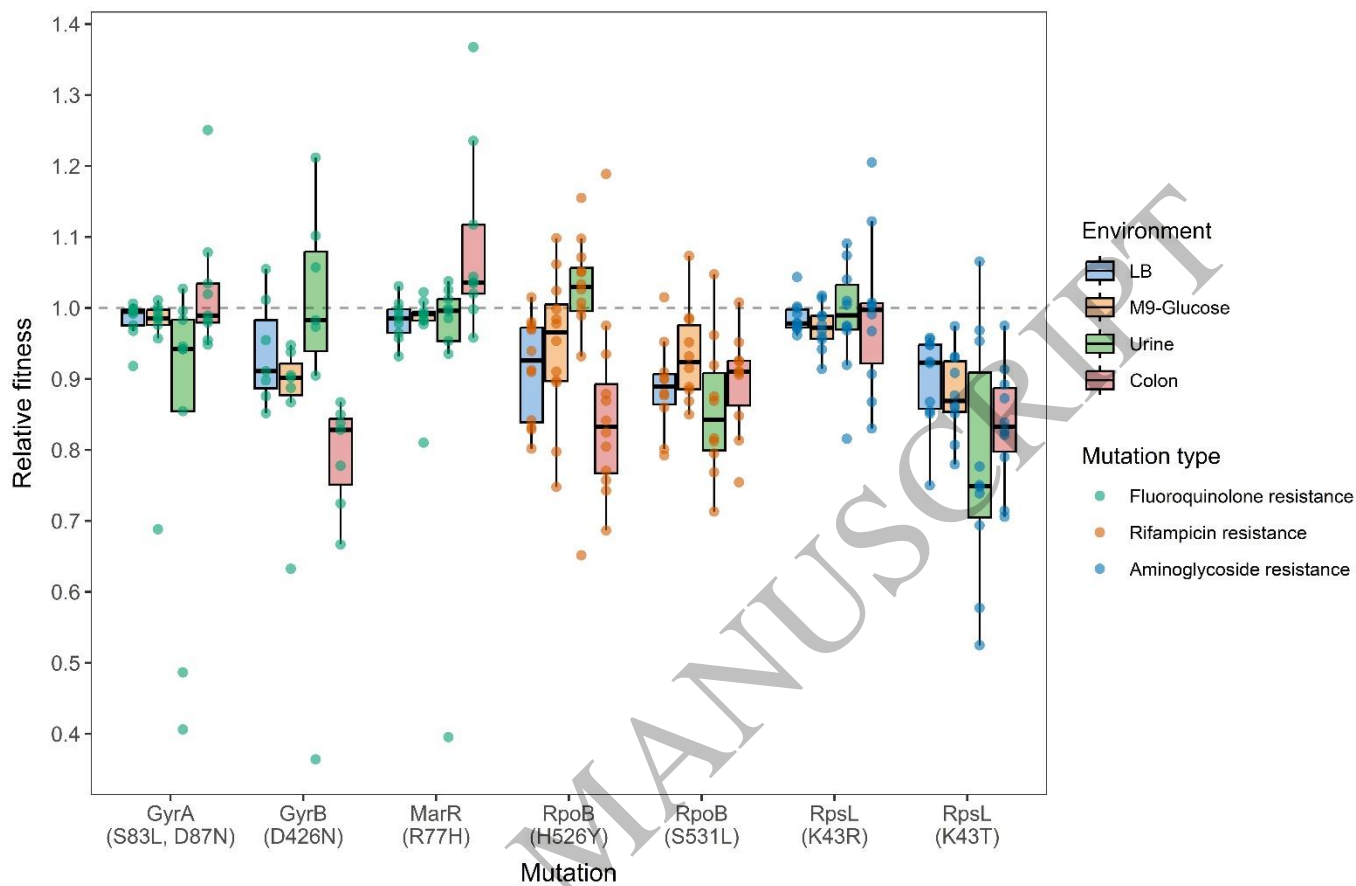


Figure 3  
182x119 mm (x DPI)

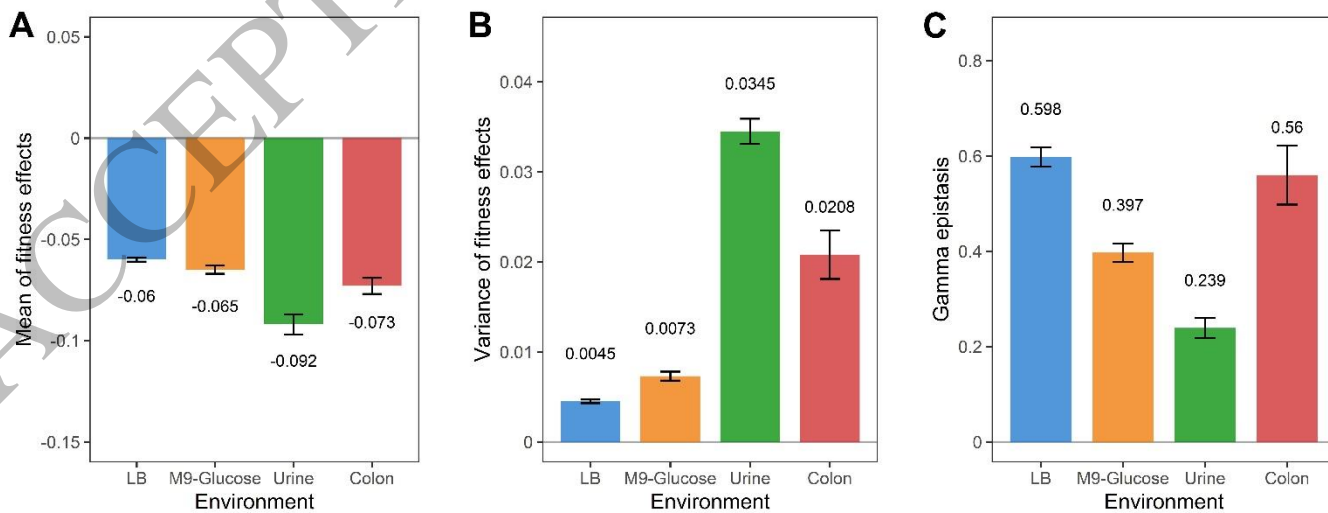


Figure 4  
182x73 mm (x DPI)

1  
2  
3  
4

5  
6  
7

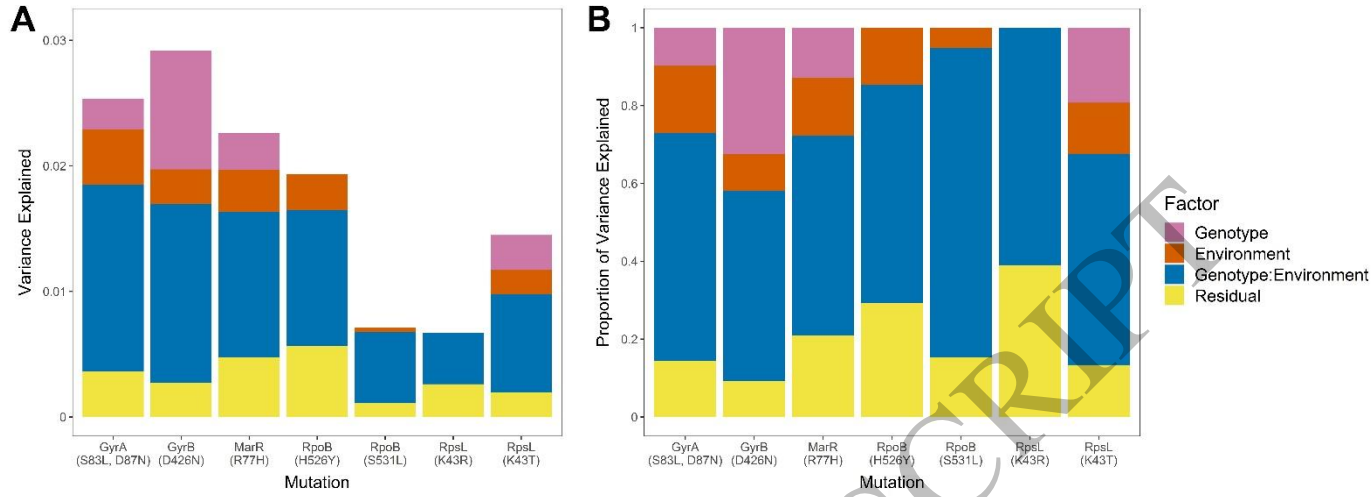


Figure 5  
182x68 mm (x DPI)

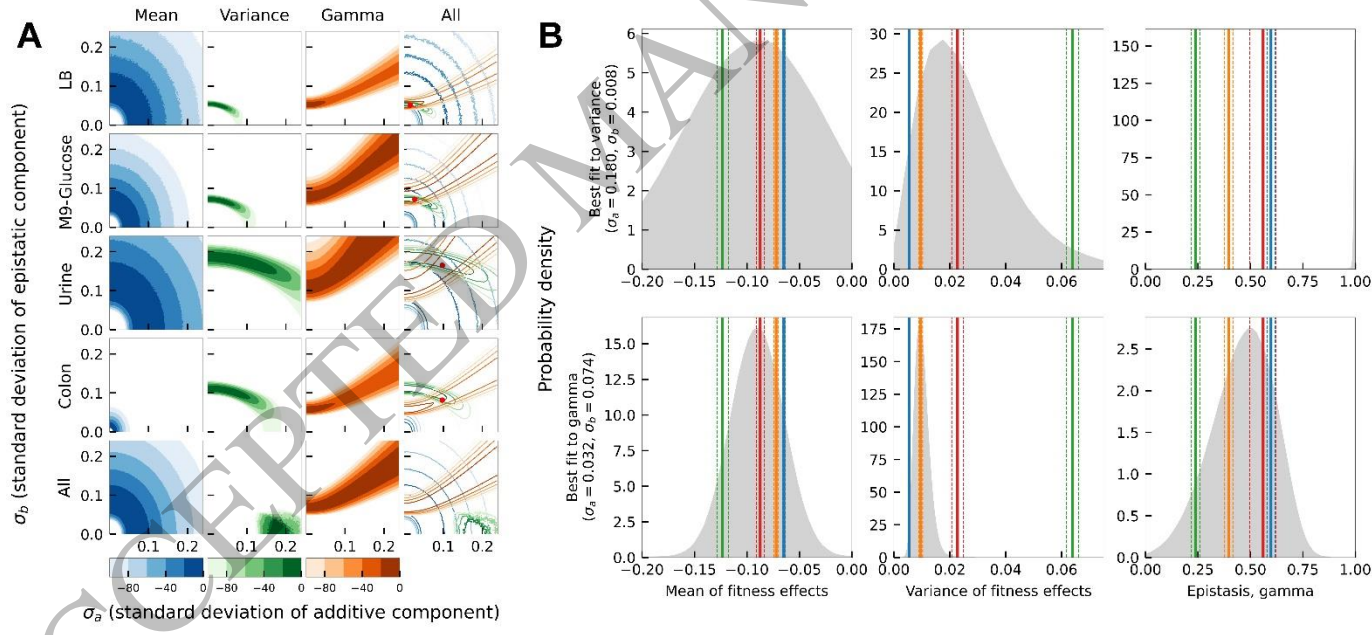


Figure 6  
182x84 mm (x DPI)

1  
2  
3  
4  
5  
6  
7  
8

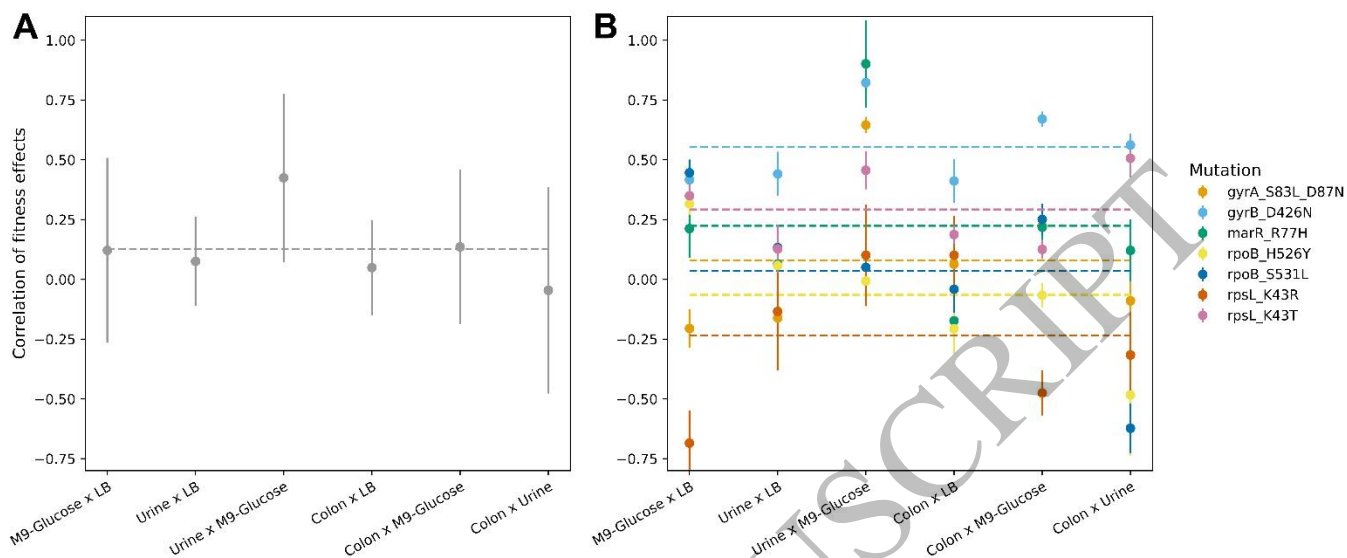


Figure 7  
182x78 mm (x DPI)

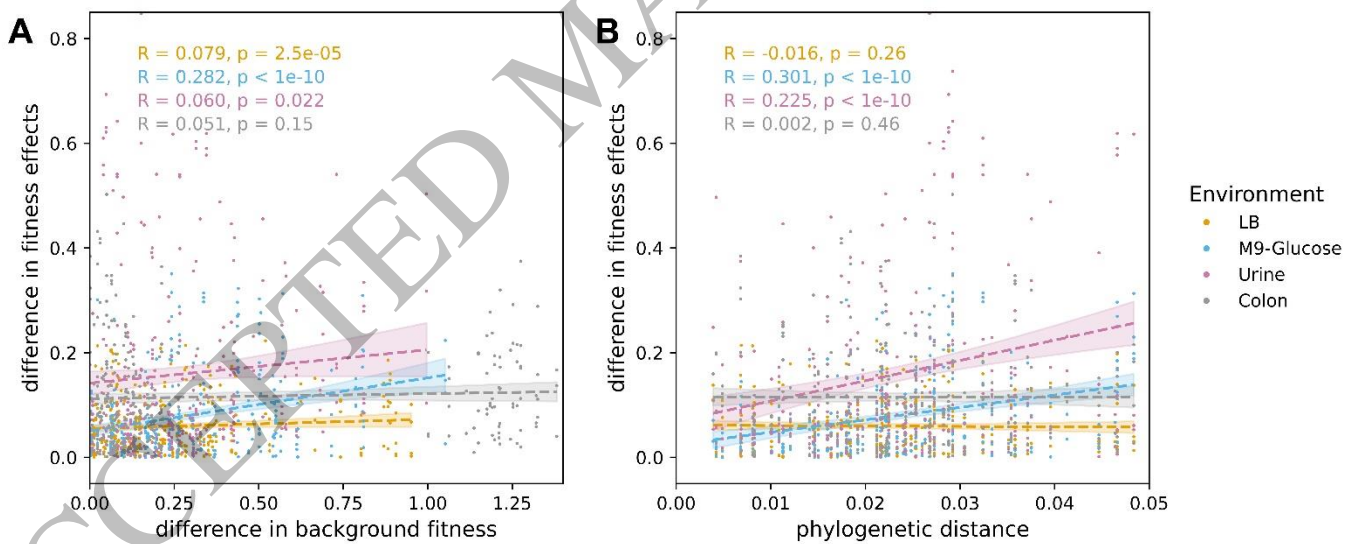


Figure 8  
182x81 mm (x DPI)